

Determining optimal COVID-19 testing center locations and capacities

Esma Akgun, Sibel A. Alumur, F. Safa Erenay*

eakgun@uwaterloo.ca, sibel.alumur@uwaterloo.ca, safa.erenay@uwaterloo.ca

Department of Management Science and Engineering, University of Waterloo, Waterloo, Ontario, Canada.

Abstract

We study the problem of determining the locations and capacities of COVID-19 specimen collection centers to efficiently improve accessibility to polymerase chain reaction (PCR) testing during surges in testing demand. We develop a two-echelon multi-period location and capacity allocation model that determines the optimal number and locations of pop-up testing centers, capacities of the existing centers as well as assignments of demand regions to these centers, and centers to labs. The objective is to minimize the total number of delayed appointments and specimens subject to budget, capacity, and turnaround time constraints, which will in turn improve the accessibility to testing. We apply our model to a case study for locating COVID-19 testing centers in the Region of Waterloo, Canada using data from the Ontario Ministry of Health, public health databases, and medical literature. We also test the performance of the model under uncertain demand and analyze its outputs under various scenarios. Our analyses provide practical insights to the public health decision-makers on the timing of capacity expansions and the locations for the new pop-up centers. According to our results, the optimal strategy is to dynamically expand the existing specimen collection center capacities and prevent bottlenecks by locating pop-up facilities. The optimal locations of pop-ups are among the densely populated areas that are in proximity to the lab and a subset of those locations are selected with the changes in demand. A comparison with a static approach promises up to 39% cost savings under high demand using the developed multi-period model.

Keywords: Location; multi-period; capacity expansion; COVID-19 testing; healthcare delivery.

Highlights

- A two-echelon multi-period location and capacity allocation model is developed.
- The model minimizes the total number of delayed appointments and collected specimens to be processed subject to budget, capacity, and turnaround time constraints.
- The model is implemented for a case study for locating COVID-19 testing centers in the Region of Waterloo, Canada.
- Managerial insights are provided to the public health decision-makers on dynamic capacity management of COVID-19 testing.
- The optimal strategy is to dynamically expand the existing specimen collection center capacities and prevent bottlenecks by locating pop-up facilities.

*Corresponding Author. E-mail address: safa.erenay@uwaterloo.ca

1 Introduction

The COVID-19 pandemic caused a significant burden to Canada with around 4,390,000 cases, 47,000 deaths, and \$275.2 billion expenditures as part of the COVID-19 economic response plan to date [23]. Several public health interventions including vaccination, testing, contact tracing, isolation of infected cases, and social distancing measures have been applied to control the spread of disease, alleviate its burden, and efficiently manage the restricted healthcare resources to fight against the COVID-19 pandemic [6, 12, 31, 49]. COVID-19 testing and surveillance is a significant part of the effort to mitigate the transmission of the disease [12, 14, 34]. The polymerase chain reaction (PCR) test is the gold standard in the diagnosis of not only COVID-19 but also several infectious diseases in the world due to its high accuracy [8, 54]. PCR testing facilitates early detection and timely isolation of COVID-19 cases, which reduces exposure of the public to the virus, and facilitates early treatment and appropriate contact management, which in turn limits disease propagation [34]. Therefore, testing is critical in every phase of the COVID-19 pandemic. The effectiveness of testing relies on fast access to testing facilities as participation in testing and surveillance depends on the accessibility to these facilities [51].

The COVID-19 testing demand changes over time depending on various factors including aggressiveness of the disease propagation, appearance of new variants, and effective implementation of public health interventions [6, 35, 49]. As observed in Ontario, during the peaks in the testing demand, the current capacity of testing centers and labs may not be sufficient to satisfy the demand [11]. These surges in the testing demand may lead to significant disruptions in operations of testing centers causing longer test turnaround times and less effective COVID-19 mitigation [9, 10]. Therefore, determining the ideal level of testing capacity in line with the varying demand prevents long waiting times, improves turnaround times, and ensures the detection and isolation of infected individuals in a timely manner. This would, in return, provide more effective pandemic control.

In the early stages of the pandemic in Ontario, asymptomatic people could get tested and there was a non-appointment-based testing system. However, with the rapid spread of the virus, the Ontario Ministry of Health (MOH), as of May 2020, prioritized those who are symptomatic or have been identified as a close contact of a confirmed case for COVID-19 testing [41]. In the summer of 2020, there was a decline in the number of COVID-19 cases and testing demand. However, with the beginning of fall, the symptoms of cold and influenza, which are similar to COVID-19 symptoms, have increased and caused significant surges in testing demand. Due to these significant surges, the capacities of the testing centers were overloaded and could not be managed well. For example, in September 2020, a drive-thru COVID-19 testing center in the city of Kitchener, Ontario was closed due to safety concerns. The cars and pedestrians waiting to get tested blocked the traffic causing a safety issue and the testing center was shut down for the day [9]. In October 2020, Ontario transitioned to appointment-based testing [40]. The MOH continually updates the testing guidelines as the pandemic evolves [41].

The capacity of COVID-19 testing is bounded by the limited number of healthcare personnel

and their working hours [14]. MOH has been increasing the testing capacity since the beginning of the pandemic based on the case count predictions from the statistical and epidemiological models developed by the Canadian COVID-19 modeling network [38]. For instance, in the first six months, testing capacity had increased from 4,000 to over 40,000 tests per day [40]. Although determining the ideal level of testing capacity in line with the varying demand is vital to use the available health resources effectively and flatten the curve, there is limited research addressing the question of when and where to implement these capacity increases.

In this paper, we study the problem of determining the optimal COVID-19 testing center locations and capacities. We develop a mathematical model based on the current testing system in Ontario, Canada. We conduct a case study for the Region of Waterloo and perform various sensitivity analyses to demonstrate the potential of the developed model and to generate insights for the public health decision-makers on dynamic capacity management of COVID-19 testing. The contributions of this paper are the development of a novel mathematical model for efficiently managing testing center location and capacity expansion decisions, which is applicable not only for COVID-19 but possibly other infectious diseases in the long term, and a case study covering the Region of Waterloo that provides valuable insights for public-health decision-makers.

The rest of the paper is organized as follows. The next section presents the relevant literature to our problem. In Section 3, we describe the current system and define the problem. We introduce the notation and the mathematical formulation in Section 4. In Section 5, we present a case study, conduct numerical analyses using real data, and discuss the implications of our numerical analyses through sensitivity analysis. We present several managerial insights in Section 6. Finally, we provide concluding remarks and discuss future research directions in Section 7.

2 Literature review

Location problems in healthcare are well-studied in the literature [3, 15, 26]. The objective functions of the healthcare facility location models depend on whose perspective is addressed as these decisions affect several stakeholders [7, 26]. For instance, from the perspective of the patients, the main objective is to improve accessibility by minimizing travel costs or travel time, waiting time at the facility, or maximizing the quality of service [26, 27, 44, 51]. On the other hand, the objective for the healthcare providers can be minimizing the operating and care costs as well as liability, while a societal perspective could consider several of these factors simultaneously [26, 55]. The most common objective function for location problems in healthcare is the proximity of the facility to demand. Some of the other common and easy to quantify objective functions in the healthcare location literature are *i*) minimization of travel costs for healthcare consumers, *ii*) maximization of covered demand, and *iii*) maximization of equity in access [26].

Ahmadi-Javid *et al.* [3] classified healthcare facility location problems based on location management purposes into two main categories: non-emergency facilities and emergency facil-

ities. According to this classification, the problem of locating COVID-19 testing centers falls under the category of non-emergency facilities and medical laboratories. Most of the papers related to non-emergency facility location problems are developed for locating primary care facilities (e.g., hospitals and clinics), and detection and prevention centers. Many of such studies focus on maximizing participation since early detection of a disease is very important for its prevention and management [16, 25, 50, 56, 57]. There are a few papers in this domain that utilize an objective function for minimizing travel time or distance as well [1, 52]. These models, however, are not applicable for locating testing centers to manage infectious diseases since they do not consider the dynamic nature of this decision problem which is essential to respond to varying demand over time due to disease propagation. On the other hand, there are studies that integrate COVID-19 testing decisions within an epidemiological framework considering disease propagation and its effects on the demand, for example, by using compartmental models such as SEIR [38, 49]. However, those studies do not address the location and capacity expansion decisions for testing centers.

The location and capacity allocation decisions of medical laboratories and testing centers are critical in terms of infectious disease prevention, management, and control, and thus, for the promotion of public health and well-being. However, the research focusing on this area is very limited [3]. Shemhaki *et al.* [46] proposed a capacitated p -median location problem for designing a network of tuberculosis (TB) testing laboratories to minimize the total transportation times of the samples. They developed a facility location and capacity allocation model that determines the optimal locations and capacities of TB testing laboratories. Their objective is to minimize the total transportation time for the samples collected daily under the budget, capacity, and maximum transportation times between any origin and laboratory constraints. They implemented their model using the data for the TB reference laboratory in British Columbia, Canada. This model considers a single-echelon setting and does not allow for dynamic capacity expansion.

The demand is assumed to be stable in most healthcare facility location models. However, testing demand for infectious diseases, such as TB and COVID-19, varies significantly over time as disease prevalence changes. To capture the variations in demand, one needs to use dynamic models that allow making time-dependent decisions for the adjustment of capacities [37]. Jena *et al.* [30] proposed a mixed-integer formulation for a generic dynamic facility location problem that allows modular capacity changes with the possibility of expansion and reduction as well as facility closing and reopening. Only a few studies address dynamic aspects of the facility location problems for primary healthcare facilities [22, 29, 36] and vaccination sites [48] using multi-period models.

In this study, we also develop a multi-period facility location model. However, different from the other multi-period facility location studies or the literature on locating non-emergency facilities and medical laboratories, in our study, we consider the design of a two-echelon system where the flow coming into the facilities to be located (i.e., the demand of people to get their

specimens collected), as well as the flow going out of the facilities (i.e., the specimens to be sent to labs for processing), are both important in terms of cost and processing times. Moreover, we model a different objective function that accounts for minimizing the weighted sum of delayed appointments and specimens and also incorporates constraints on the turnaround time which is imperative in testing infectious diseases.

The waiting time of specimens is an important factor that needs to be considered in the calculation of turnaround times. Our model considers both the waiting time of specimens after collection as well as the waiting time due to congestion at labs. Most studies on location of prevention centers incorporate congestion into their formulations using queuing models [18, 45, 56–58]. In our study, we model time delay due to congestion at the labs with a generic function that depends on the capacity utilization of each lab and incorporate this delay in processing times at the labs into the turnaround time constraint [4]. For computational efficiency, we then use a piecewise linear function to model the delay in processing times at the labs due to congestion as it is known that piecewise linear functions can be a reasonable approximation for non-linear functions [19, 20, 52].

To the best of our knowledge, only a limited number of studies focus on locating COVID-19 testing centers [32, 33]. Li *et al.* [32] proposes a bi-objective parallel machine scheduling-location model to optimize the design of massive COVID-19 testing programs. The objectives of this model are to minimize the makespan and total traveling distance while determining the location of testing sites as well as assigning and scheduling the tested communities. The authors apply their model to real-world data from the city of Wuhan, China. The proposed model is not a multi-period model, hence, dynamic changes in the testing demand over time are not modeled. Zhang *et al.* [55] study a related problem on vaccination site selection, appointment acceptance and assignment, and scheduling decisions for mass vaccination. Liu *et al.* [33] determines the locations of testing centers and dynamically adjusts their capacities for a case study in China, where these testing facilities can be opened only in the first period during the planning horizon. The COVID-19 testing system modeled in these existing studies is quite different than the integrated network in Ontario which requires a two-echelon structure and where testing capacity can be adjusted by expanding the capacities of the existing centers as well as by opening pop-ups over the entire planning horizon. Moreover, these studies do not incorporate constraints on test turnaround times nor consider congestion and delays in the facilities providing COVID-19 testing services.

To conclude, there is not any study in the literature that simultaneously addresses the dynamic aspect of location decisions in a two-echelon setting considering capacities, budget, congestion, and turnaround times. Hence, the developed model is different than the traditional facility location models as it incorporates several aspects that are specific to the system being modeled.

3 System description and problem definition

Ontario’s public health system includes several provincial organizations and local public health units (PHUs) that work in collaboration as described in Figure 1. The MOH makes strategic decisions to promote and manage health care delivery and public health by developing legislation, regulations, and policies. The Ministry is responsible for funding and maintaining a sustainable health system by ensuring that it satisfies the needs of people in Ontario [42]. Within the Ministry, the Office of Chief Medical Officer of Health (CMOH) identifies the provincial public health needs, determines the public health strategies, and controls the public health programs delivered by Ontario’s local PHUs. The CMOH reports directly to the Ontario Deputy Minister of Health. Based on the strategies and policies developed by the CMOH, PHUs provide an efficient community health program focusing on disease prevention, control of infectious diseases, and surveillance at the local level and lead to execute these provincial strategies. Public Health Ontario (PHO) provides scientific and technical information and expertise to MOH, CMOH, and local PHUs to help with their decisions and actions [42]. Moreover, PHO conducts laboratory testing for several diseases and supports other organizations in Ontario’s public health system in case of an emergency or outbreak. Ontario Health (OH) helps create an integrated public health system for Ontario by coordinating and connecting the aforementioned provincial health agencies to ensure better health care delivery. Its main task is to oversee the health care system, suggest improvements, and provide support for other agencies when needed [42].

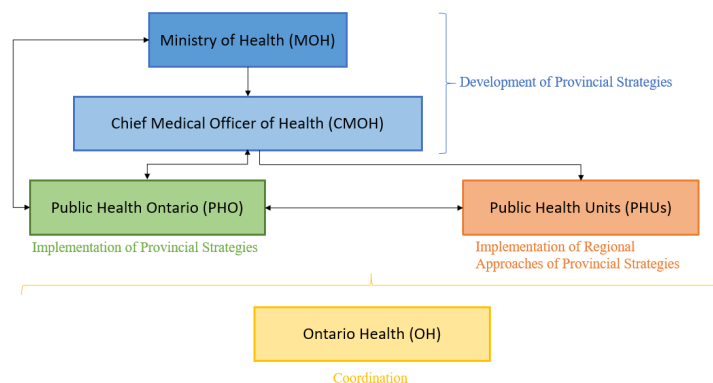


Figure 1: Overview of Ontario Public Health System.

As detailed above, there are several different stakeholders involved in the healthcare system of Ontario (i.e., MOH, CMOH, PHUs, PHO, and OH). COVID-19 testing is delivered through an integrated network via the collaboration of these stakeholders. Given the complex nature of the Ontario healthcare system, in the next subsection, we first present an overview of the system delivering COVID-19 testing and explain the roles of these different organizations in this process. We then define the problem on hand in Section 3.2.

3.1 Overview of the current COVID-19 testing process

Ontario has developed the COVID-19 testing network to manage specimen collection, transportation and logistics, laboratory analysis, and reporting of the results. Figure 2 describes the structure of the COVID-19 testing network in Ontario. In this network, the MOH administers the overall testing strategy. By tracking the spread of COVID-19, MOH makes strategic decisions and deploys resources as needed. CMOH provides testing guidance which is developed and updated based on the recommendations from a testing strategy expert panel coordinated by PHO. OH coordinates specimen collection, transportation and routing, lab processing, and reporting. OH also helps with the procurement of testing supplies and distribution of them to assessment centers and hospitals. In addition, OH works with the MOH to expand the provincial lab network’s capacity. Lastly, PHUs handle contact tracing and case management. PHUs also help with the decisions regarding the assessment centers based on local needs [39].

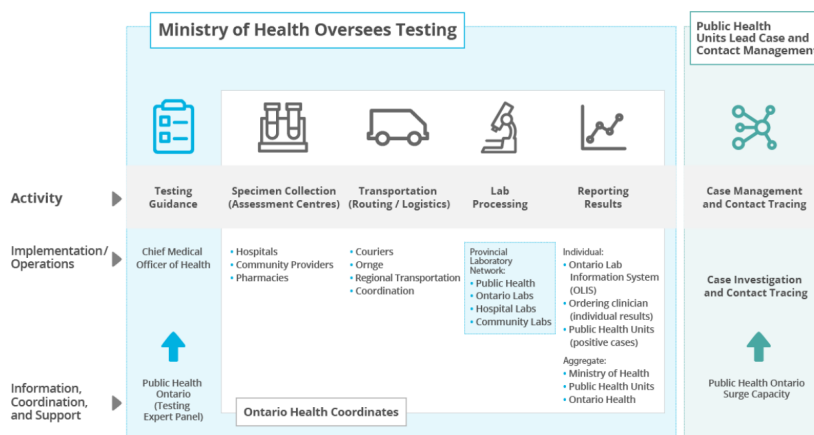


Figure 2: COVID-19 Testing Network in Ontario [39].

The process of COVID-19 testing for an individual patient or specimen in Ontario is explained in the process flow diagram depicted in Figure 3. The red dashed boxes in this figure represent the waiting times of individuals or specimens throughout the testing process. Specimens are collected from the individuals at *assessment centers*, which include hospitals, pharmacies, drive-thrus, and mobile pop-up centers. Since all assessment centers in Ontario serve by appointment only, the individuals who want to get tested first need to book an appointment through the web portal or by phone.

The specimens for PCR testing are collected from the individuals during their appointments at the assessment centers. After the collection, the specimens are sent from the assessment centers to the labs using couriers. The specimens from each assessment center are sent to a lab that is best positioned to analyze the results in a reasonable time, e.g., within two days. The specimens may need to wait at the assessment centers as they are sent to the lab in batches. The waiting time depends on how frequently the assessment center sends the collected specimens to the lab. The *turnaround time* of the specimens, which is the amount of time it takes for test results to be available after specimens are collected, varies based on the location and

transportation schedule of assessment centers, proximity to the lab performing the PCR testing as well as the workload of the lab. The regional transportation coordination system organizes the routing and logistics across the province to achieve the targeted turnaround times.

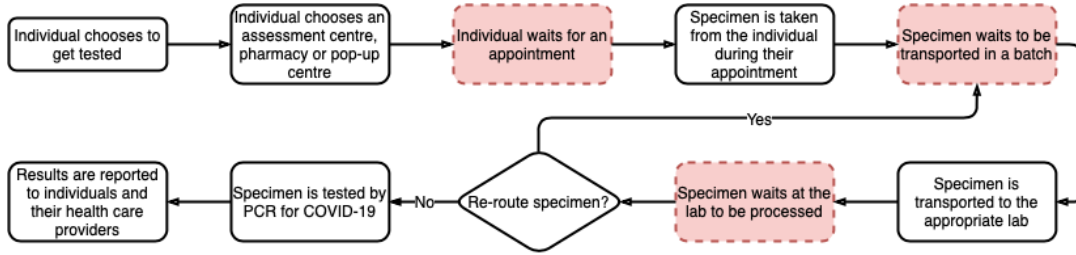


Figure 3: COVID-19 testing process flow diagram (red dashed boxes represent waiting times).

The specimens are analyzed within the provincial laboratory network consisting of PHO, hospital, and community labs. When the specimens arrive at a lab, they may wait to be processed depending on the congestion in the lab. However, if the lab is at its capacity, the specimens may be rerouted to another lab with available capacity. Therefore, directing the specimens to the labs with sufficient capacity is important to balance the workload at the labs, limit the additional transportation cost, and reduce time spent due to the rerouting of the specimens, which may increase the turnaround times.

After the specimens are processed, the lab results are posted in the Ontario Lab Information System (OLIS) and become available in the Government of Ontario’s results portal for individuals and attending clinicians to access them confidentially [39]. If the test result is positive, it is shared with the local PHU, which initiates contact tracing and case management. OH coordinates this integrated system of specimen collection, transportation, lab processing, and reporting to provide timely turnarounds. Their aim is to achieve a target of delivering 80% of the test results within two days of specimen collection.

There are several potential issues related to the performance of the current system. During peak demand, the assessment centers may have insufficient specimen collection capacity (not enough appointments per day) which may cause delayed testing of individuals at risk and, in return, increased risk of spreading the virus. Such bottlenecks can be avoided by preemptively expanding the capacities of the existing centers or deploying additional pop-up testing centers. However, there is no systematic approach to determine when and where to deploy these pop-up centers and how much to increase the capacity of the existing ones.

Another important concern is related to the flow of specimens from assessment centers to the labs. There may be several labs that can be highly congested during peak demand times which would necessitate the rerouting of many specimens to other labs that may, in turn, result in significant delays in the turnaround time. The rerouting of the specimens might be prevented by dynamically assigning assessment centers to the labs with available capacity and anticipating the effects of congestion on the turnaround time in advance. To address these issues, optimize flows, and reduce inefficiencies in this current system, we define and model a new multi-period

location and capacity allocation problem as detailed in the next section.

3.2 Problem definition

We consider a two-echelon facility location and capacity allocation problem that determines optimal locations and capacities of testing (assessment) centers in Ontario over a finite planning horizon. The model analyzes the province of Ontario as being separated into 523 forward sortation areas (FSAs); i.e., geographical units based on the first three characters in a Canadian postal code. Ontario has a total of 34 PHUs and each FSA is assigned to a local PHU. Each PHU contains and coordinates several assessment centers including hospitals, pharmacies, and drive-thrus that perform COVID-19 testing. Although a single FSA may include multiple assessment centers, we represent this situation in the model as if there exists a single assessment center with a capacity equal to the total capacity of the existing centers in that FSA.

We assume, as validated by the MOH, that assessment centers can collect specimens from FSAs contained in their PHUs. Collected specimens are then processed at the labs which belong to the COVID-19 provincial diagnostic network. Although some patients may prefer to travel to specimen collection centers offering an earlier appointment in other PHUs, this effect would be negligible as our model aims to minimize the total number of delayed appointments.

During the peaks in the testing demand, the capacities of the assessment centers may be overloaded, and the testing demand may not be satisfied on time (i.e., the target turnaround time may be exceeded). This can be avoided by expanding the capacity of existing assessment centers or opening new pop-up centers. For the existing centers, the timing of the capacity expansions and the expanded capacities need to be decided. The capacity of the existing assessment centers can be increased by a certain percentage of the existing capacity selected from a discrete set of alternatives, e.g., 10% or 25% of their existing capacity.

For opening new pop-up centers, the locations of these centers have to be determined. MOH arrange pop-up testing centers to be opened temporarily to increase accessibility to testing during the peaks in the testing demand. These facilities are typically located in the parking lots of community centers and are housed in buses, with a standard number of public health workers, doctors, or nurses on staff. That is, each pop-up center's capacity is standard and fixed. However, pop-up testing centers can be opened and closed more than once during the planning horizon. Each FSA represents a candidate location for a pop-up testing center. MOH wants every FSA to have a testing center located within a reasonable distance (e.g., walking distance for downtown Toronto, or within the same PHU).

In the multi-period setting, the planning horizon is assumed to be finite and divided into discrete and equally sized periods. The timings of the operations considered in the model (e.g., waiting time for transportation and test processing times) are measured in terms of the number of periods they take. The decisions of opening pop-up centers and capacity expansion for the existing ones are implemented at the beginning of periods. In addition, the specimens are collected at the beginning and sent to the labs at the end of given periods.

The processing of the specimens, from collection to the compilation of the PCR test results, needs to be completed within a given turnaround time that includes transportation and waiting times, and other delays. In particular, since each assessment center sends its specimens to a particular lab at specific periods, specimens may need to wait at the assessment centers until they are sent to a lab. Moreover, the congestion at the labs might delay the processing of the specimens which might, in turn, affect the target turnaround times. Hence, the effect of congestion at labs is incorporated into the problem as well. To sum up, the turnaround times of the specimens depend on the waiting time at the assessment center, transportation time from the center to the lab, processing time at the lab, and delay in processing due to congestion at the lab.

We reasonably assume that the congestion level at each lab depends on the percentage utilization of its capacity. We additionally assume a first-in-first-out (FIFO) policy to serve the testing demand and process specimens, i.e., the delayed appointments and specimens are served or processed in the first successive available period. Accordingly, the waiting time to get an appointment is at most one period if there is enough capacity in the succeeding period.

The turnaround time, which is the amount of time it takes for the test results to be available after specimens are collected, does not consider the time between requesting an appointment and providing a sample for the PCR test. We incorporate this factor in the objective function by minimizing the total number of delayed appointments and ensuring that the required capacity increases are done to minimize the time people wait until their sample is collected. Furthermore, as detailed in the previous section, there might be a delay in processing specimens at the labs. Therefore, for the objective function of our problem, we minimize the weighted sum of delayed appointments and specimens.

An alternative objective function is to find the minimum required budget to serve a specified demand level by limiting the total number of delayed appointments and specimens, which we also consider and model in this study. We would like to note that other alternative objective functions, such as minimizing the total waiting time or minimizing the maximum travel distance may be also applicable to the considered problem. However, the public decision-makers in our setting prefer to incorporate these performance metrics through a turnaround time and maximum travel distance constraint.

To conclude, these system dynamics and targets constitute a problem of determining *i*) the optimal number and locations of pop-up centers to open, *ii*) the capacities of existing assessment centers to be expanded, *iii*) assignment of demand regions to the assessment centers, and *iv*) the assignment of specimens to the labs to minimize the weighted sum of delayed appointments and specimens subject to capacity, budget, turnaround time, and maximum travel distance constraints.

4 Model formulation

In this section, we first introduce the required parameters and decision variables and then present a mathematical formulation of the problem detailed in the previous section.

Sets

- K : Set of PHUs.
- I_k : Set of FSAs contained in PHU $k \in K$.
- J_k^e : Set of locations of *existing* specimen collection centers under PHU $k \in K$.
- J_k^n : Set of potential locations for *new* pop-up centers under PHU $k \in K$.
- J_k : $J_k^e \cup J_k^n$.
- L : Set of labs.
- Q_j : Set of available capacity increments for existing center $j \in J_k^e$ (e.g., 10%, 25%, 50%).
- T : Set of time periods in a discrete and finite planning horizon.
- T_j : Set of time periods that the specimen collection center $j \in J_k$ sends the collected specimens to the lab, where $T_j \subseteq T$.
- \hat{T}_j : $T_j \cup \{0\}$, where $\hat{T}_{j\tau}$ corresponds to the τ^{th} element of the set, $\tau = \{1, \dots, |\hat{T}_j|\}$.

Parameters

- d_{it} : Testing demand of FSA $i \in I_k$ in period $t \in T$.
- D_{jl} : Distance between specimen collection center $j \in J_k$ and lab $l \in L$.
- L_k : Maximum travel distance for PHU $k \in K$.
- C_{jt}^e : Capacity of the existing center located in $j \in J_k^e$ in period $t \in T$.
- C_j^n : Capacity of the pop-up center to be located in $j \in J_k^n$.
- C_{lt} : Capacity of lab $l \in L$ in period $t \in T$.
- tp_l : Processing time of specimens in lab $l \in L$.
- t_{jl} : Transportation time of specimens from center $j \in J_k$ to lab $l \in L$.
- tw_{jt} : Maximum number of periods that specimens sent to a lab in period $t \in T_j$ wait in the collection center $j \in J_k$.
- Δ : Target turnaround time for specimens.
- $h(\cdot)$: Congestion function that represents the waiting time of the specimens at the lab.
- f_j : Fixed cost of operating a pop-up center in location $j \in J_k^n$ per period.
- g_{qjt} : Fixed cost of expanding the capacity of existing center $j \in J_k^e$ by $q \in Q_j$ in period $t \in T$.
- c : Variable operating cost of a testing center per person.
- v : Unit transportation cost of specimens from collection centers to labs (unit cost per distance).
- B : Available budget over the planning horizon.
- a_{ij} : Indicator specifying if center located in $j \in J_k$ can cover FSA $i \in I_k$, where

$$a_{ij} = \begin{cases} 1, & \text{if } D_{ij} \leq L_k, k \in K, i \in I_k, j \in J_k, \\ 0, & \text{otherwise.} \end{cases}$$
- α : The weight of the total number of delayed appointments in the objective function.
- β : The weight of the total number of delayed specimens in the objective function.

Decision Variables

- $y_{jt} = \begin{cases} 1, & \text{if a pop-up center is opened in location } j \in J_k^n \text{ in period } t \in T, \\ 0, & \text{otherwise.} \end{cases}$
- $z_{qjt} = \begin{cases} 1, & \text{if the capacity of existing center located in } j \in J_k^e \text{ is expanded by } q \in Q_j \\ & \text{in period } t \in T, \\ 0, & \text{otherwise.} \end{cases}$
- $\omega_{jlt} = \begin{cases} 1, & \text{if center } j \in J_k \text{ sends specimens to lab } l \in L \text{ at the end of period } t \in T_j, \\ 0, & \text{otherwise.} \end{cases}$

- x_{ijt} = Number of people from FSA $i \in I_k$ served by specimen collection center $j \in J_k$ in period $t \in T$.
 u_{jlt} = Number of specimens that is sent from center $j \in J_k$ to lab $l \in L$ at the end of period $t \in T_j$.
 s_{it} = Number of delayed appointments from FSA $i \in I_k$ in period $t \in T$.
 r_{lt} = Number of delayed specimens in lab $l \in L$ in period $t \in T$.
 γ_{lt} = Capacity utilization rate of lab $l \in L$ in period $t \in T$.

Based on this notation, the mathematical model that minimizes the weighted sum of delayed appointments and specimens is formulated as follows:

$$\min \quad \alpha \sum_{k \in K} \sum_{i \in I_k} \sum_{t \in T} s_{it} + \beta \sum_{l \in L} \sum_{t \in T} r_{lt} \quad (1)$$

$$s.t. \quad s_{i(t-1)} + d_{it} = s_{it} + \sum_{j \in J_k} x_{ijt} \quad k \in K, i \in I_k, t \in T \quad (2)$$

$$x_{ijt} \leq a_{ij} d_{it} \quad k \in K, i \in I_k, j \in J_k, t \in T \quad (3)$$

$$\sum_{i \in I_k} x_{ijt} \leq C_j^n y_{jt} \quad k \in K, j \in J_k^n, t \in T \quad (4)$$

$$\sum_{i \in I_k} x_{ijt} \leq C_{jt}^e + \sum_{q \in Q_j} q C_{jt}^e z_{qjt} \quad k \in K, j \in J_k^e, t \in T \quad (5)$$

$$\sum_{q \in Q_j} z_{qjt} \leq 1 \quad k \in K, j \in J_k^e, t \in T \quad (6)$$

$$\sum_{i \in I_k} \sum_{t=\hat{T}_{j\tau}+1}^{\hat{T}_{j(\tau+1)}} x_{ijt} = \sum_{l \in L} u_{jl}(\hat{T}_{j(\tau+1)}) \quad k \in K, j \in J_k, \tau = \{1, \dots, |\hat{T}_j| - 1\} \quad (7)$$

$$\sum_{l \in L} \omega_{jlt} = 1 \quad k \in K, j \in J_k, t \in T_j \quad (8)$$

$$u_{jlt} \leq \mathcal{M} \omega_{jlt} \quad k \in K, j \in J_k, l \in L, t \in T_j \quad (9)$$

$$\sum_{k \in K} \sum_{j \in J_k} u_{jl(t-t_{jl})} + r_{l(t-1)} = C_{lt} \gamma_{lt} + r_{lt} \quad l \in L, t \in T \quad (10)$$

$$(tw_{jt} + t_{jl} + tp_l) \omega_{jlt} + h(\gamma_{l(t+t_{jl})}) \leq \Delta \quad k \in K, j \in J_k, l \in L, t \in T_j \quad (11)$$

$$\sum_{k \in K} \left(\sum_{t \in T} \left(\sum_{j \in J_k^n} f_j y_{jt} + \sum_{q \in Q_j} \sum_{j \in J_k^e} g_{qjt} z_{qjt} + \sum_{i \in I_k} \sum_{j \in J_k} c x_{ijt} \right) + \sum_{j \in J_k} \sum_{l \in L} \sum_{t \in T_j} v D_{jl} u_{jlt} \right) \leq B \quad (12)$$

$$y_{jt} \in \{0, 1\} \quad k \in K, j \in J_k^n, t \in T \quad (13)$$

$$z_{qjt} \in \{0, 1\} \quad k \in K, q \in Q_j, j \in J_k^e, t \in T \quad (14)$$

$$\omega_{jlt} \in \{0, 1\} \quad k \in K, j \in J_k, l \in L, t \in T_j \quad (15)$$

$$x_{ijt}, s_{it} \geq 0, \text{ integer} \quad k \in K, i \in I_k, j \in J_k, t \in T \quad (16)$$

$$u_{jlt} \geq 0, \text{ integer} \quad k \in K, j \in J_k, l \in L, t \in T_j \quad (17)$$

$$0 \leq \gamma_{lt} \leq 1 \quad l \in L, t \in T \quad (18)$$

The objective function (1) minimizes the weighted sum of the number of delayed appointments and delayed specimens over the planning horizon. Constraints (2) guarantee patient flow balance in consecutive periods. The sum of the number of delayed appointments from the previous period and the demand in the current period must be equal to the number of people who get tested plus the number of delayed appointments in the current period. Constraints (3) assure that people in each FSA can get tested only if there is a testing center within a certain travel distance. Constraints (4) and (5) are the capacity constraints for pop-up and existing specimen collection centers, respectively. Constraints (6) specifies that at most one capacity level can be selected for existing centers at each time period.

Constraints (7) ensure the flow balance of specimens between specimen collection centers and the labs. The total inflow which is the total number of specimens that are collected at a center must be equal to the total outflow which is the total number of specimens that are sent from that center to a lab at that time period. At the specimen collection centers, the specimens wait to be sent to a lab and the waiting time depends on the frequency that the center sends collected specimens to the lab. Thus, at each time period, the total number of specimens that are sent to the lab will be the sum of the specimens waiting until that time period.

Constraints (8) specify that each specimen collection center sends specimens to a single lab at each time period. Constraints (9) together with constraints (8) ensure that a specimen collection center does not send any specimen to a lab unless it sends all specimens to that lab. Constraints (10) ensure the specimen flow balance in consecutive periods at the labs. The sum of the total number of specimens that are sent to a lab and the leftover specimens from the previous period must be equal to the sum of the processed and delayed specimens at that lab in the current period.

Constraints (11) make sure that the turnaround times of specimens do not exceed the target turnaround time. If a center sends its specimens to a lab, the sum of the waiting time of specimens at the center, transportation time to the lab, processing time at the lab and time delay due to congestion should not exceed the target turnaround time. Constraints (12) ensure that the total cost of operating pop-up centers, expanding the capacity of existing centers, the operational cost of testing and the transportation cost of specimens to the labs do not exceed the available budget. Finally, constraints (13)-(18) define the domains of the decision variables.

We would like to note that even though capacity expansion and pop-up location decisions are defined for each period, such an overly dynamic solution may not be easy to implement in practice. The model can readily be modified to ensure that capacity expansion or location decisions can be implemented only in certain periods. For example, those decisions can be defined in the first period of each day or only for specific periods, i.e., for a set of particular time periods that is a subset of T . Furthermore, if specific actions are not allowed for a certain PHU, FSA, or location, the values of the corresponding decision variables can be pre-set to zero before solving the model. Hence, the model is generic enough to accommodate such restrictions. We refer the readers to Section 5.2.4 for an analysis reporting the performance of a less dynamic

and more practical form of testing decisions.

In the above model, in constraints (11), we use a non-decreasing generic congestion function which depends on the capacity utilization at the lab. Let us now assume the congestion function $h(\cdot)$ is a piecewise linear function specified by its breakpoints (b^m, δ^m) as shown in Figure 4. The capacity utilization of a lab can then be represented as a convex combination of two consecutive breakpoints [19, 20, 52]. The b^m and δ^m values can be obtained through expert opinion (as done in our case study) or by fitting a piecewise linear function to the actual congestion curve. To formulate the model using such a piecewise linear congestion function, we introduce the following additional notation:

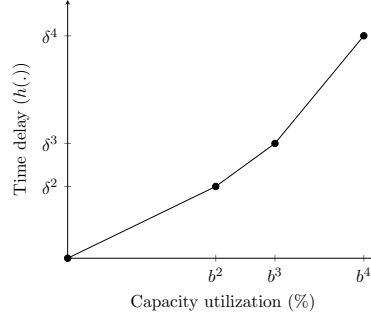


Figure 4: Piecewise linear congestion function.

M : Set of congestion levels considered for the labs.

b_l^m : Capacity utilization of lab $l \in L$ corresponding to the congestion level $m \in M$ (e.g., 80%, 100%).

δ_l^m : Waiting time of specimens in lab $l \in L$ corresponding to the congestion level $m \in M$.

In addition to the above parameters, we define a new set of binary variables and convex combination multipliers:

$$\phi_{lt}^m = \begin{cases} 1, & \text{if utilization of lab } l \in L \text{ is between } b_l^m \text{ and } b_l^{(m+1)}, m \in M, \text{ in period } t \in T, \\ 0, & \text{otherwise.} \end{cases}$$

λ_{lt}^m =Convex combination multiplier corresponding to b_l^m for lab $l \in L, m \in M$ in period $t \in T$.

The model is then formulated as an MILP as follows:

$$\min \quad (1)$$

$$s.t. \quad (2) - (18)$$

$$\gamma_{lt} = \sum_{m \in M} \lambda_{lt}^m b_l^m \quad l \in L, t \in T \quad (19)$$

$$h(\gamma_{lt}) = \sum_{m \in M} \lambda_{lt}^m \delta_l^m \quad l \in L, t \in T \quad (20)$$

$$\sum_{m \in M} \lambda_{lt}^m = 1 \quad l \in L, t \in T \quad (21)$$

$$\lambda_{lt}^1 \leq \phi_{lt}^1 \quad l \in L, t \in T \quad (22)$$

$$\lambda_{lt}^m \leq \phi_{lt}^{(m-1)} + \phi_{lt}^{(m)} \quad l \in L, t \in T, m = 2, \dots, |M| - 1 \quad (23)$$

$$\lambda_{lt}^{|M|} \leq \phi_{lt}^{(|M|-1)} \quad l \in L, t \in T \quad (24)$$

$$\sum_{m=1}^{|M|-1} \phi_{lt}^m = 1 \quad l \in L, t \in T \quad (25)$$

$$\phi_{lt}^m \in \{0, 1\} \quad l \in L, t \in T, m = 1, \dots, |M| - 1 \quad (26)$$

$$\lambda_{lt}^m \geq 0 \quad l \in L, t \in T, m \in M \quad (27)$$

Constraints (19)-(25) determine two consecutive breakpoints of the congestion function that the capacity utilization of the lab lies between, and incorporate the corresponding time delay due to the congestion. Constraints (19) represent the utilization of lab capacity as a weighted average of breakpoints.

By constraints (20), the time delay corresponding to the congestion level at a lab is determined depending on the capacity utilization of that lab using the convex combination multipliers enforced by constraints (19). Constraints (21) ensure that multipliers add up to one. Constraints (22)-(25) impose the restrictions that all $\lambda_{lt}^m = 0$ except for one consecutive pair, i.e., λ_{lt}^m and λ_{lt}^{m+1} . Lastly, constraints (26) and (27) specify the domains of the variables.

Instead of introducing the binary variable ϕ_{lt}^m and constraints (22)-(26), we can define λ_{lt}^m as a special ordered set of type 2 (SOS2) variables which enforce that at most two λ_{lt}^m can be positive. We refer to the formulation with objective function (1), constraints (2)-(21), (27) and with SOS2 variables as the *min-delay* formulation.

The min-delay formulation minimizes the weighted sum of delayed appointments and specimens under a given budget. An alternative modeling approach is to find the minimum required budget to achieve a specific performance level in terms of targeted delayed appointments and specimens. In that case, the decision-maker needs to solve the model for given values of s_{it} and r_{lt} with the below objective function, which will be referred to as the *min-cost* formulation:

$$\min \sum_{k \in K} \left(\sum_{t \in T} \left(\sum_{j \in J_k^n} f_j y_{jt} + \sum_{q \in Q_j} \sum_{j \in J_k^e} g_{qjt} z_{qjt} + \sum_{i \in I_k} \sum_{j \in J_k} c x_{ijt} \right) + \sum_{j \in J_k} \sum_{l \in L} \sum_{t \in T_j} v D_{jl} u_{jlt} \right)$$

We develop two objective functions, i.e., *i*) minimizing a weighted sum of delayed appointments and specimens and *ii*) minimizing the total cost of designing and operating the testing system, and utilize them both in solving this problem. Both of these optimization problems are NP-hard as they can be reduced to the well-known *uncapacitated facility location problem* which is also NP-hard [21].

In particular, to solve our problem, we propose the following solution scheme. We first solve the min-delay formulation under a given budget and obtain the optimal values of the decision variables of the delayed appointments and specimens. Then, for these given values that are

obtained by solving the min-delay model, say \bar{s}_{it} and \bar{r}_{it} , we solve the min-cost formulation to determine the minimum budget required to meet given values of delayed appointments and specimens. Alternatively, the two objective functions could be combined by incorporating a penalty cost for delayed appointments and specimens. The resulting problem can then be solved under a single objective function minimizing the total cost. In the next section, we present the application of the model in a case study from Ontario, Canada.

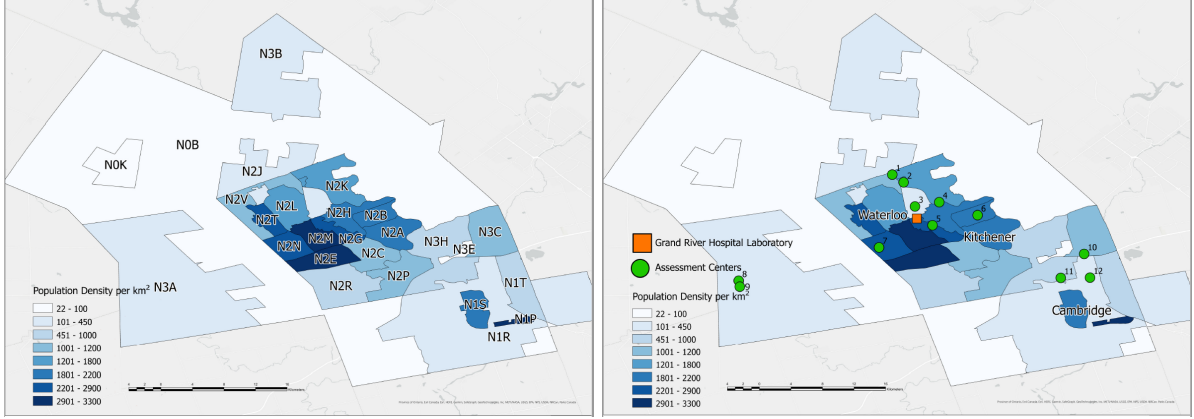
5 Computational results

In our numerical analysis, we apply the developed model to facilitate access to COVID-19 testing in the Region of Waterloo (RoW) PHU in Ontario using real data and derive practical insights for the decisions and policies around the timing and locations of the required capacity expansions. *All data regarding this case study is publicly shared [13].* Throughout our computational analysis, we first solve the model with the min-delay objective function using a loose budget constraint to obtain the minimum delayed appointments and specimens, and then minimize the required budget given these values. As there are enough potential sites for pop-ups and capacity expansion opportunities, we are able to obtain an optimal solution with no delayed appointments under a sufficient budget, i.e., $s_{it} = 0$ for all $i \in I$ and $t \in T$. In our analysis, we focus on finding the minimum required budget to ensure no delayed appointments unless stated otherwise. The mathematical model is solved using CPLEX 20.1.0 to optimality. All analyses are performed on a computer with a 2.3 GHz Intel processor and 8 GB RAM, running on macOS 10.15.7.

5.1 RoW case study

5.1.1 Input parameters

The RoW is a mid-sized community including three cities located in southwestern Ontario (i.e., Cambridge, Kitchener, and Waterloo) with a population of around 630,000 people. Figure 5a shows the population density map of 26 FSAs in the RoW. Currently, the RoW has 12 assessment centers including hospitals (Grand River, St Mary’s General, and Cambridge Memorial Hospitals), drive-thrus, and pharmacies that perform COVID-19 testing in the PHU (Figure 5b). There is a single lab operated by the Grand River Hospital (GRH) that processes the specimens collected at the assessment centers. The frequencies of sending specimens to the labs, the congestion levels, the current capacities of the assessment centers and the lab are obtained through interviews with the public health officials from the RoW. We consider a one-week planning horizon divided into 4-hour long periods. The one-week planning horizon is reflective of MOH’s frequency of providing a report on COVID-19 assessment and reviewing the need for updating public health interventions [43]. We assume that opening pop-up testing centers and capacity expansion decisions are made daily, i.e., at the beginning of each day. We assign a greater value to the delayed appointments in the objective function (i.e., $\alpha > 0.5$) to ensure no delayed appointments under the expanded testing capacity given a sufficient budget.



(a) FSAs in the Region of Waterloo.

(b) Assessment centers and the lab in the Region of Waterloo.

Figure 5: Locations of the FSAs, the assessment centers, and the lab in the RoW.

The appropriateness of the planning horizon, frequency of the decisions, and weight values are approved by MOH.

We calculate the shortest traveling distances between FSA pairs using Python code and OpenStreetMap API. The maximum travel distance is taken as 20 km; i.e., there should be a testing center within 20 km of each FSA for individuals to get tested. Through our discussions with the MOH, we concur that 20 km is a reasonable maximum travel distance for RoW where parking spaces are widely available and affordable. The processing time of specimens and target turnaround time are taken as 4 hours and 2 days, respectively, in line with the current practice [39]. We obtain the variable component of the operational cost from clinical studies estimating costs and human resources needed for several testing strategies [12]. Since some costs were confidential and are not publicly available, we estimate the fixed cost of operating pop-up testing centers and capacity expansion costs considering the capital cost of a mobile clinic and the salaries of the medical staff.

We derived the data on daily COVID-19 testing demand from the public reports of the MOH presenting the daily number of people tested in each PHU [24]. Since we consider FSAs in terms of the smallest geographic unit in our model, we assign each FSA’s testing demand proportional to its population. The appropriateness of this practice is also verified during our discussions with the MOH. Figure 6a shows the 7-day averages of the number of tests completed in the RoW PHU over a year. To analyze the model outcomes under different demand scenarios, we choose three separate weeks each from December 2020, April 2021, and August 2021 that correspond to high, medium, and low demand intervals, respectively. The corresponding demand values for these three different weeks are shown in Figure 6b.

5.1.2 Case study results

We solve the model using the parameters introduced in the previous section for three different demand levels. Figure 7a–7c presents the maps indicating the optimal locations and timing of

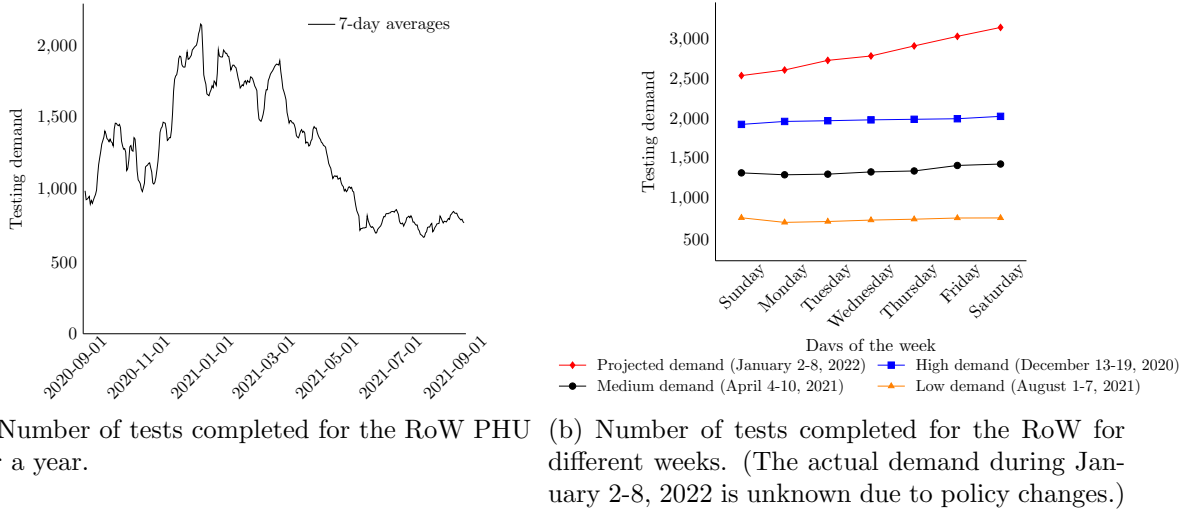


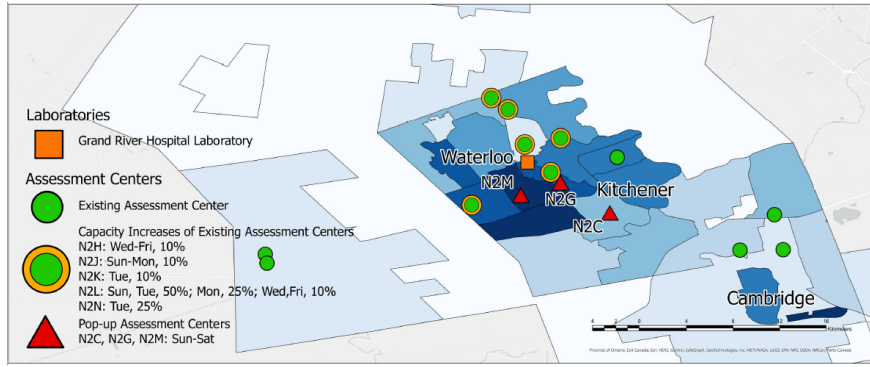
Figure 6: Testing demand for the RoW.

required capacity expansions to satisfy all testing demand on time for high, medium, and low demand weeks, respectively, based on the model solutions. The legends of the maps show the timing of the capacity adjustments. For instance, for the medium-demand week in April, the model suggests opening two pop-up testing centers one in N2C and the other in N2G, where the second one is not operated on Thursday.

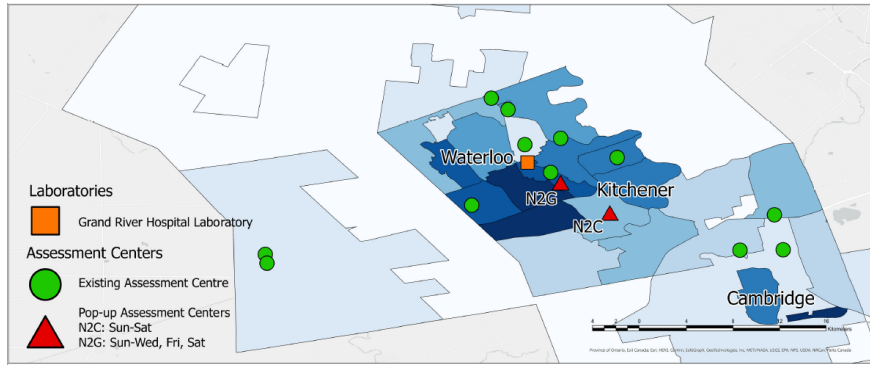
Figure 7 shows that the developed model locates pop-up testing centers close to the lab to reduce the transportation cost of specimens from the assessment centers to the lab. Most of the capacity expansions are in existing centers located in densely populated areas that are close to the lab due to the same reason. The model dynamically changes the capacities of the existing centers to address the slight increases in demand at a minimum cost. In addition, the model opens pop-up centers in the south, southwest, and southeast sides of the lab (see Figure 7a). The first two location choices may be related to high population intensity in those sections of the regions (i.e., around FSAs N2M and N2G). The last one could be explained by the lack of an existing assessment center to serve the medium-populated area between the southeast side of the lab and the city of Cambridge. Those insights are verified under higher demand scenarios as well (see Figure 8).

Another vital observation from Figure 7 is that, for the medium and low demand weeks, only a subset of the pop-up centers selected in the high demand week was opened. This indicates the possibility that varying demand would only change the number of additional pop-up centers to be opened and not their locations. Based on this observation, the RoW PHU can determine a set of stable pop-up center locations to be opened/closed depending on the pandemic load.

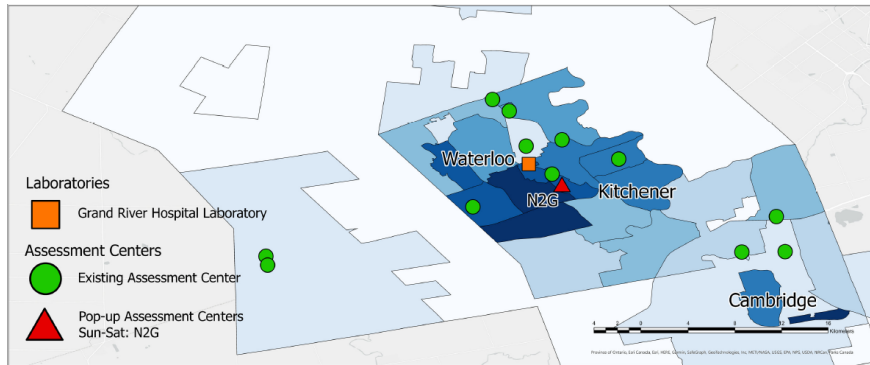
To test everybody in the medium and low demand week, the need for the capacity increase is addressed only through the use of pop-up centers. The model prefers opening pop-up testing centers rather than expanding the capacity of the existing ones due to the lower unit cost of testing at pop-ups; i.e., the unit cost of opening a pop-up testing center is lower than the unit cost of expanding the capacity of an existing one. For instance, for the high demand



(a) High demand week (December 13-19, 2020)



(b) Medium demand week (April 4-10, 2021)



(c) Low demand week (August 1-7, 2021)

Figure 7: The optimal locations and timings of capacity expansions for high, medium, and low demand weeks.

week, 49.2% of testing demand is satisfied by pop-up centers while only 2.1% is satisfied by the capacity increase in the existing centers.

5.1.3 Case study with projected demand

Although we evaluate the performance of the developed model retrospectively based on realized demand, the model can be used for prospective analysis with forecasted testing demand. To illustrate the potential of the model for prospective analysis, we focus on the post-Omicron period of the pandemic, which provides an ideal scenario for evaluating the extreme demand case. Following the emergence of the Omicron variant, the burden of COVID-19 on the health system has reached its highest levels since the beginning of the pandemic [5]. As a result, the

significant increase in the workload on the assessment centers overloaded the existing capacities and individuals could not book a COVID-19 test appointment promptly [17].

During this period, Canada has lost sight of the true size of the pandemic as the highly infectious Omicron variant overwhelmed the testing capacity [35]. MOH updated the guidance on PCR testing for COVID-19. Due to an unprecedented case volume and limited testing capacity, PCR testing was prioritized for those most vulnerable to COVID-19. A large portion of mild cases and exposures could not be tested, and these cases were not recorded. This eventually led to discrepancies in the reported numbers and real-time data. Since testing numbers can no longer be relied upon to accurately reflect the case count of COVID-19 in Ontario, we project the demand for testing using a forecasting model and analyze the continuation of PCR testing for everyone.

We developed an autoregressive integrated moving average (ARIMA) model to forecast the testing demand for the RoW after the emergence of the Omicron variant. ARIMA is a forecasting model that uses time-series data to predict the future values in the series [47]. We built the ARIMA model in Python using the historical data from November 1 until December 24 as the transmission of the Omicron variant in Ontario was high during that time and forecasted the testing demand for the week of January 2, 2022. The projected demand values are shown in Figure 6b in comparison to the demand patterns used in the previous analyses (low, medium, high). We then solve the developed model using the projected demand values to evaluate the model performance under an extreme case. The locations and timings of capacity expansions required to test everybody on time with the projected demand values are presented in Figure 8.

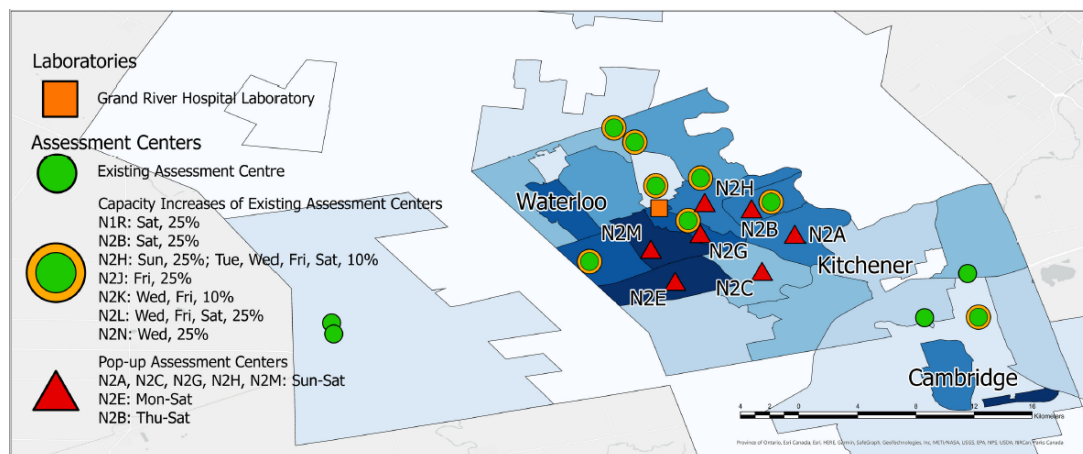


Figure 8: The locations and timings of capacity expansions with the projected demand values.

With the surge in the number of cases due to the Omicron variant, the model assigned more than twice as many pop-up centers to the RoW as it does for the high demand scenario in December (see Figure 8). Similarly, the capacity expansion for the existing testing centers is also much higher in Figure 8 compared to those in Figure 7. Like those in Figure 7, the model opened pop-up assessment centers around the lab to reduce transportation costs and better serve the highly populated areas around the lab. The majority of pop-up centers are opened in

the south of the lab because there are no existing assessment centers on that side of the region except three assessment centers way down southeast around the city of Cambridge. The model did not open any new locations to the north of the lab as the capacities of existing centers are enough to cover the demand there.

Unlike the capacity expansion plans for the base case, the model outcomes propose a more composite plan dynamically utilizing pop-up centers and capacity expansion in existing centers at a higher level than for the high demand case of December. To cover the majority of the demand during this interval, the model first opens five pop-up centers on Sunday and uses a 25% capacity expansion of the existing assessment centers to cover the residual demand. To address the increasing demand, the model opened an additional pop-up center on Monday and increased the capacities in several existing centers until Thursday. After that, since they become costlier, the model reduced the capacity expansions and opened an additional pop-up center instead. Figure 8 verifies our earlier observation that the pop-up locations at lower demand scenarios are subsets of those for higher demand scenarios, i.e., the pop-up centers opened for the high demand case of December 2020 are also opened for the extreme demand scenario of January 2022.

5.1.4 *Case study with uncertain demand*

Although the developed model assumes that the testing demand over the planning horizon is known, it reflects the current decision-making process in the MOH. Public health decision-makers make capacity decisions periodically for upcoming weeks, as formulated in our model, using the projected demand values obtained from epidemiological models following a rolling horizon approach [38, 49]. However, the actual demand is unknown, thus, the performance of the actual and proposed capacity expansion plans may suffer from this uncertain nature of the pandemic. Therefore, we would like to evaluate the performance of our model under uncertainty.

For this purpose, we first solve our model using projected demand values and then evaluate the resulting solutions under the realized demand. In particular, we first forecast the testing demand for high, medium, and low demand weeks using the ARIMA model based on testing demand of the preceding 8 weeks as described in Section 5.1.3. We then solve the developed model using these projected demand values to find the optimal pop-up locations and required capacity increases to test everybody on time. Next, we fix the optimal locations and capacity decisions obtained under the projected demand and evaluate whether the decisions of the proposed model are still effective under the realized demand. The results are presented in Table 1.

In Table 1, the rows labeled as “Projected” present the outcomes of the optimal model using projected demand values from the ARIMA model. On the other hand, the performance metrics in rows labeled as “Realized” are obtained by minimizing the total cost under the realized demand where the timing and locations of capacity expansions are set to those obtained from the optimal solution using the projected demand values. The third column of the table presents the total demand values for both the projected and realized demand corresponding to each week.

Table 1: Model outputs under projected and realized demand scenarios.

Demand set	Scenario	Total demand	Delayed appointments (%)	Avg utilization of pop-ups (%)	Avg utilization of existing centers (%)	Total cost(\$)
December (high)	Projected	13,631	0.0	81.5	68.8	843,572
	Realized	13,933	0.0	81.8	74.9	861,302
April (medium)	Projected	8,677	0.0	78.1	45.9	537,038
	Realized	9,508	0.0	74.7	55.5	585,760
August (low)	Projected	5,414	0.0	89.6	38.5	331,348
	Realized	5,231	0.0	89.8	36.5	320,672

The performances are compared based on the percentage of the population whose appointments are delayed to the next day, utilization of testing resources, and total cost.

Table 1 illustrates that the projected and realized performances are very close to each other. Specifically, when the plan with projected data is applied under the realized demand, it still guarantees timely service of all testing demand, i.e., zero percent delayed appointments, in all three demand sets. The deviation of the actual demand from the projected values results in small differences in the average utilization of pop-ups and existing centers and the total cost. In high and medium demand weeks, the average utilization rate and total cost evaluated using the realized demand values are higher than those for the projected demand because the realized demand during these weeks exceeds the projected demand. Testing more individuals with the same capacity leads to increases in the total cost and average utilization of testing centers. These results indicate that the solutions obtained with projected demand can satisfy the actual demand in a timely manner without creating significant variations from the anticipated resource utilizations and total cost.

We also test the model under random demand scenarios. We generate three different scenarios for each week using a normal distribution with a mean and standard deviation of the realized demand values over that week. We first solve the model using realized demand values and then fix the locations and timings of capacity expansions. Next, we solve the model under each random demand scenario. The total demand values for each scenario and corresponding results are presented in Table 2.

Table 2: Model outputs under realized and random demand scenarios.

Demand set	Scenario	Total demand	Delayed appointments (%)	Avg utilization of pop-ups (%)	Avg utilization of existing centers (%)	Total cost(\$)
December (high)	Realized	13,933	0.0	80.9	71.3	864,513
	Random 1	13,968	0.0	81.1	71.2	864,524
	Random 2	13,901	0.0	81.4	69.4	862,825
	Random 3	13,980	0.0	81.7	71.2	866,753
April (medium)	Realized	9,508	0.0	76.3	58.5	583,731
	Random 1	9,774	0.1	76.3	58.7	583,733
	Random 2	9,338	0.0	76.8	56.8	573,759
	Random 3	9,532	0.3	76.7	61.7	599,358
August (low)	Realized	5,231	0.0	89.3	37.3	320,672
	Random 1	5,186	0.0	89.9	36.7	323,942
	Random 2	5,295	0.0	89.9	36.8	324,409
	Random 3	5,287	0.0	89.5	36.1	318,047

When the solution with the realized data is evaluated under random demand scenarios, all

demand is served in a timely manner for the majority of the cases with a very small portion ($< 1\%$) of delayed demand, in particular, for the scenarios of the medium demand week. The differences in the average utilization of pop-ups and existing centers, and total cost are caused by the deviation of the realized demand from the randomly generated demand values and are not significant. These results demonstrate that the developed model leads to high-quality solutions, which are robust under demand uncertainty, for the case study.

5.2 Sensitivity analysis

Input parameters including the number of candidate locations for pop-up centers, weights of delayed appointments and specimens in the objective function, available budget, length of the planning horizon, testing demand, and maximum travel distance may significantly affect the model outcomes. Hence, in this section, we present detailed sensitivity analyses to evaluate the effects of these parameters on the results.

We first assess the scalability of our model and solution potential with the commercial solver CPLEX on larger problem instances. Our base case problem instances with 26 candidate locations (i.e., FSAs) were solved to optimality by CPLEX in 41.8, 20.0, and 1.2 seconds for high, medium, and low demand weeks, respectively, using the default settings. We generated larger problem instances by doubling, tripling, and quadrupling the number of candidate locations, i.e. 52, 78, and 104 candidate locations. Under the three demand scenarios (high, medium, and low) and three new problem sizes, we tested nine additional problem instances by setting a time limit of two hours to CPLEX. Two instances out of three demand scenarios with 52 candidate locations were solved to optimality in 21 and 405 seconds. We observed that CPLEX was able to produce very high-quality solutions within two hours of run time for the remaining problem instances achieving average optimality gaps of 0.05%, 0.40%, and 0.16% with 52, 78, and 104 node instances, respectively. Accordingly, for larger problem instances, our results show that decision-makers can employ off-the-shelf solvers with reasonable time limits to obtain good-quality solutions.

5.2.1 *The relative importance of delayed appointments and specimens*

The model with the min-delay objective minimizes the weighted sum of delayed appointments and specimens. The decision-maker can assign relative weights to the delayed appointments and specimens based on their importance when using the current model. For the case study presented in Section 5, we assigned a higher weight to the delayed appointments since the laboratory capacity was not a limiting factor in Ontario as the delayed specimens are rerouted and processed at the labs with the available capacity within the provincial laboratory network. To assess the trade-off between the two objectives, we now test the model with different weight coefficients assigned to the delayed appointments (α) and specimens ($\beta = 1 - \alpha$). The results for various α values under high-, medium-, and low-demand scenarios are presented in Figure

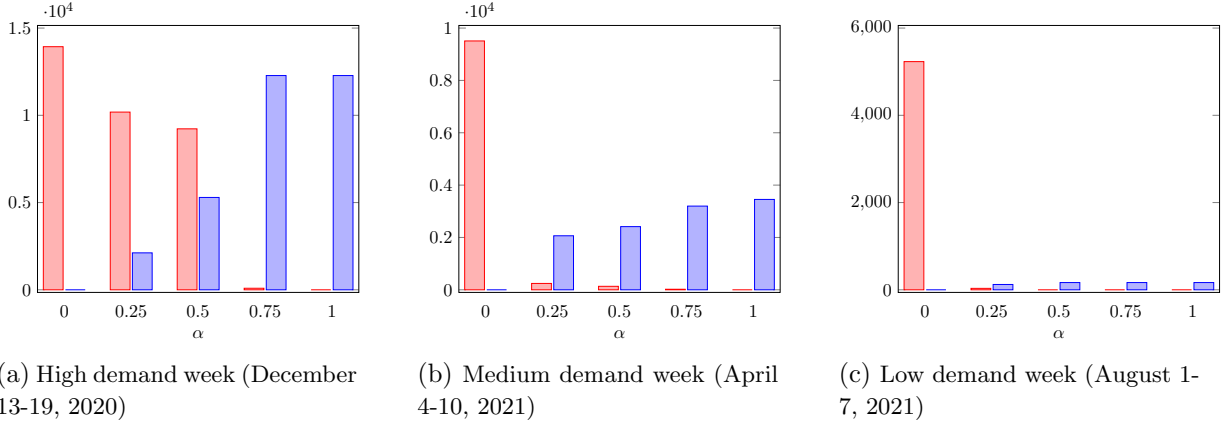


Figure 9: Number of delayed appointments (red) and delayed/rerouted specimens (blue) based on different weights in the objective function.

9.

When the weight of delayed appointments is greater than that of delayed specimens (i.e., when $\alpha > 0.5$), the model allocates most of the budget towards capacity expansion to test as many people as possible. As expected, when the objective weight of delayed appointments reaches zero, the model suggests testing nobody to minimize the number of delayed specimens. This confirms that assigning a weight of zero to delayed appointments would not yield meaningful results in practice. The marginal effect of increasing the weight α in reducing the number of delayed appointments is significant during the weeks with high demand; however, this marginal effect diminishes when demand decreases. The results of this analysis suggest that incorporating lab capacity as an additional decision variable may be desired for effectively managing high-demand scenarios, and can be a promising direction for future research.

5.2.2 Available budget

The model with the min-cost objective finds the minimum total cost required to test everyone on time. We now conduct further analysis to evaluate the impact of budget on the percentage of total demand receiving delayed appointments. We use the low demand week in August to perform the analysis. The results are presented in Table 3. The first column of Table 3 shows the available budget as a percentage of the minimum required budget to test everyone on time. The second column indicates the percentage of total demand receiving a delayed appointment. The third, fourth, fifth, and sixth columns specify the average number and utilization of pop-up testing centers opened, average capacity expansion, and utilization of the existing centers, respectively. Finally, the last column reports the solution time of the model.

The results in Table 3 demonstrate that at least one pop-up center should be opened in order not to have any delayed appointments. Even though existing testing centers are not fully utilized, a pop-up is required to test everyone due to the maximum travel distance requirement as there is no testing center within 20 km of several FSAs. Moreover, the delayed appointments gradually decrease to 6% at a similar rate as the budget increases up to 90% of the base case,

Table 3: Solutions for different values of the available budget using low demand week in August.

Available Budget (%)	Delayed appointments (%)	Avg # of opened pop-ups	Avg utilization of pop-ups opened (%)	Avg capacity expansion for existing centers (%)	Avg utilization of existing centers (%)	Solution time (sec)
10	90	0	0	0	3.4	1.7
20	79	0	0	0	10.3	2.2
30	69	0	0	0	16.6	6.3
40	58	0	0	0	24.3	55.3
50	48	0	0	0	28.4	92.7
60	37	0	0	0	35	72
70	27	0	0	0	41.3	8.4
80	16	0	0	0	47.7	90.7
90	6	0	0	0	53.1	684.13
100 (Base case)	0	1	89.3	0	37.3	1.2

Table 4: Comparison of the performances of the multi-period and static models.

Instance number	Demand set	Planning horizon	Static model			Multi-period model		
			Testing cost (\$)	Capacity increase cost* (\$)	Solution time (sec)	Testing cost (\$)	Capacity increase cost* (\$)	Solution time (sec)
1		1-week	778,871	48,972	10	778,900	47,892	25.3
2	December	2-week	1,591,177	107,408	38.3	1,591,516	99,876	143.9
3	(high)	3-week	2,407,966	190,848	50.7	2,410,576	155,968	184.5
4		4-week	3,097,054	254,464	55.5	3,101,338	190,984	224.7
5		1-week	553,952	31,808	4.2	554,208	29,628	41.6
6	April	2-week	1,118,646	63,616	34.7	1,120,328	52,556	89.6
7	(medium)	3-week	1,637,944	95,424	61.1	1,641,131	69,428	126.1
8		4-week	2,091,696	127,232	111.7	2,095,515	91,572	106.7
9		1-week	304,776	15,904	1.1	304,776	15,904	1.5
10	August	2-week	626,260	31,808	1.3	626,260	31,808	1.3
11	(low)	3-week	956,066	48,384	2.2	956,091	47,744	1.6
12		4-week	1,293,080	63,616	3.4	1,293,080	63,616	2.5

*Capacity increase refers both to opening pop-up centers and expanding the capacity of existing ones.

beyond which the reduction in delayed appointments is quite limited. This indicates that, if feasible, 90% of the base case budget could be an ideal solution for reducing the delayed appointments cost-efficiently. When 90% of the minimum required budget is used, no pop-up center is opened, and existing centers could test 94% of the people on time.

5.2.3 *The value of the multi-period model*

In this section, we analyze the potential benefits of using a multi-period model. We perform this analysis under four different planning horizons (i.e., one, two, three, and four weeks) with low, medium, and high-demand scenarios, which constitute a total of 12 instances. We first solve a static model assuming that the decisions of opening the pop-up testing centers and expanding the capacity of existing ones are made once at the beginning of the planning horizon and remain the same thereafter. We then solve the multi-period model by making the decisions of capacity increases at the beginning of each day as in our previous analyses. We compare the total costs of testing people, opening pop-up testing centers, and expanding the capacity of existing ones using static and multi-period models. The results are presented in Table 4 and Figure 10.

In most of the solutions presented in Table 4, the static and multi-period models incur similar testing costs, which constitute the majority of the total cost. This is because testing cost mainly depends on the number of people to be tested, which is the same in both models. The slight differences are due to the change in transportation costs that depend on the proximity of the specimen collection centers to the lab.

The total cost associated with the multi-period model is usually less than that of the static one as the former incurs significantly less costs for opening pop-ups and expanding the capacity of existing centers under high and medium demand scenarios. Observe from Figure 10 that the savings in the costs of capacity expansion and opening pop-ups with the multi-period model, compared to the static one, can be up to 39%. In more than half of the instances with high and medium demand scenarios, the associated cost savings are above 20%. For the instances with low demand scenarios, on the other hand, the savings in costs are insignificant. The multi-period model dynamically determines the locations and timings of the capacity expansions considering the fluctuation in the testing demand. Therefore, the new pop-up centers are opened and the capacities are expanded exactly when they are needed throughout the planning horizon, rather than the more costly option of implementing all these changes at the beginning for the whole planning horizon as done by the static model.

Our results show that there can be considerable savings in total costs of opening pop-up centers and capacity expansions by using the developed multi-period model. However, the multi-period model can be harder to implement in practice due to the need to frequently change decisions regarding the facilities. In this context, it is important to note that the differences between the costs of the multi-period and static models are not as much for the instances with a 1-week planning horizon (Table 4). The good performance of the static one-week policy should not be interpreted as limited room for improvement but as an opportunity. This result, which

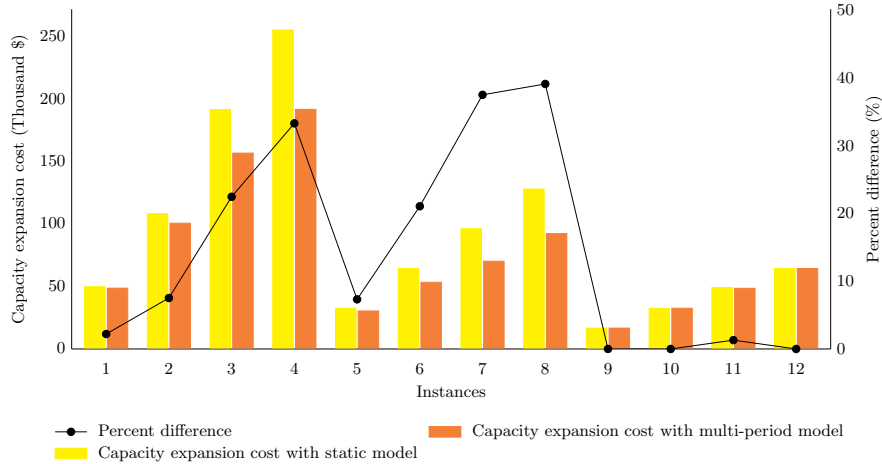


Figure 10: The value of multi-period model on different instances.

is possible to obtain thanks to the developed model, implies that making COVID-19 testing center location and capacity expansion decisions weekly can be more practical and equally cost-efficient compared to making these decisions on a day-by-day basis. On the other hand, public health decision-makers should avoid implementing static decisions for more than one week as this may incur extra costs to the system.

5.2.4 Testing demand and maximum travel distance

We also test our model under different demand values and provide details of our results in Supplementary Materials. We consider the low, medium, and high demand weeks from Section 5.1 as base cases and increase the corresponding demands by up to 50% with 10% increments. For the low demand week, compared to the base case, the model does not open additional pop-up testing centers until the demand is increased by 50%, i.e., the increase in testing demand can be served by using the base case pop-up center and expanding the capacity of the existing assessment centers. For medium and high demand weeks, the average number of opened pop-up testing centers increases with demand.

The maximum travel distance is taken as 20 km for the base case scenarios. Since this parameter affects the numbers and locations of pop-up testing centers, we additionally solve the model using different maximum travel distance values (will be referred to as L) for each demand scenario to capture its effect on the model output. Moreover, this distance could be lower for particular regions with limited parking space. Therefore, we test for $L \in \{5, 10, 15, 20, 25, 30\}$. When the maximum travel distance increases, more people can get access to testing from a particular existing or pop-up testing center. This results in the opening of fewer pop-up testing centers, as existing capacity can be better utilized to serve remote demand, as well as an increase in the average utilization of the opened pop-ups. On the other hand, when the maximum travel distance decreases, more pop-up testing centers are needed which leads to lower utilization of some pop-up testing centers.

6 Managerial Implications

Our model and analyses provide practical plans and valuable insights for public health decision-makers to dynamically manage testing center capacity for COVID-19 in response to the evolving needs of the pandemic. The primary objective of the MOH is to ensure that the necessary capacity increases are made to test everybody on time with limited resources. Thus, the decision-makers must consider conflicting interests and balance the trade-off between total cost and total demand receiving delayed appointments. The formulation with a min-delay objective allows decision-makers to minimize the total demand receiving delayed appointments considering the capacity, and turnaround time limitations for a given budget. By setting the budget to the right level, the decision-makers can use the proposed model to minimize delayed appointments cost-effectively. This way, the proposed model can be used to meet the requirements of all stakeholders and balance their competing interests by efficiently using the available resources.

It is essential to consider the travel distance of people tested, which is an indicator of accessibility to COVID-19 testing. Our model addresses this by incorporating a maximum travel distance and ensuring that everyone has access to a testing center within a specified range. The maximum travel distance (MTD) depends on various factors, including the demographical and spatial features of the considered region. For instance, a longer MTD may be suitable in rural areas, while a shorter MTD may serve better in metropolitan areas. Our model captures the effect of traveling distance on the utilization of testing capacity and use capacity extension decision to promote accessibility to COVID-19 testing services. Therefore, public health decision-makers can also utilize the proposed model as a tool to design a more accessible COVID-19 testing network under various MTD scenarios.

Our results show that as the COVID-19 load in the population increases, it is optimal to place the majority of the testing load on pop-up centers and utilize existing centers to cover incremental demand increases between the openings of pop-up centers. This is mainly because pop-up centers have lower unit costs of increasing testing capacity and provide locational flexibility. This implies that public health decision-makers may rely on opening pop-up centers to increase their specimen collection capacity as their primary response to increasing demand for testing, while increasing existing testing center capacities may be a secondary option to avoid the lump sum costs. Pop-up testing centers should be particularly considered in densely populated FSAs with limited nearby existing testing centers.

Our results further imply that while developing a testing capacity expansion plan (either as an emergency response strategy before a new pandemic or planning during a new one), decision-makers can identify a predetermined set of locations for pop-up centers using the proposed model. Subsequently, a subset of these locations can be opened in a particular order based on the fluctuations in demand to cover various demand increase scenarios (e.g., a steady increase in infection load due to infection spread or a much faster one due to an emerging virus variant). Moreover, when selecting the locations of pop-up centers or determining the capacity expansion of existing centers, their proximity to the labs should be considered to minimize the

transportation costs of specimens.

Lastly, it is important to consider the frequency of capacity expansion decisions in terms of both cost and practicality. The dynamic nature of the proposed model requires making decisions regarding testing center locations and capacity expansions on a day-by-day basis. This level of adaptability may pose challenges in terms of logistics, coordination, and resource management. By adopting an appropriate frequency of decision-making approach, decision-makers can find a balance between cost-efficiency and practicality. Our analysis suggests that weekly decisions can be practical and equally cost-efficient compared to daily decisions.

7 Conclusions

In this paper, we study a facility location and capacity allocation problem for COVID-19 testing motivated by the public health system in Ontario, Canada. We develop a mathematical model to determine the optimal timing and locations of pop-up testing centers, capacity expansions for the existing centers, assignment of demand regions to centers, and the assignment of specimens to the labs under budget, capacity, and turnaround time constraints. We propose two different objective functions that can be used based on the needs of the healthcare system and the perspectives of the public health decision-makers. The first objective is to minimize the weighted sum of delayed appointments and specimens, while the second objective is to minimize the total cost under a given acceptable value of delayed appointments and specimens.

We implement the developed model in a case study from the Region of Waterloo public health unit using real data and conduct several numerical experiments. The results of our analysis provide insights into optimal locations and capacities of testing centers, the timing of capacity expansions, and the benefit of improving testing performance in Ontario. In our results, opening pop-up centers is preferred over capacity expansion due to their flexible locations and lower unit costs of testing. In the optimal solutions, pop-up centers cover the major load when testing demand is high, but existing centers are preferred to cover incremental increases between two pop-up openings. We observe that there is a preferred set of pop-up locations in the optimal solutions and the model generally opens a subset of those locations with the changes in demand. The model strategically locates pop-ups or expands the capacity of existing centers around the lab to reduce transportation costs. Moreover, pop-ups tend to be located in densely populated FSAs with limited existing centers.

Our numerical experiments with retrospective data help identify the bottlenecks in COVID-19 testing and provide strategies and insights to overcome them. In addition, we show that the developed model can be combined with prediction methods and used as a decision-aid tool for proactively determining the need for capacity increases based on the estimated new COVID-19 cases. Such a decision aid tool can be quite useful for public health decision-makers to design effective and dynamic COVID-19 testing strategies against new COVID-19 variants (e.g., Omicron, Delta, BA.5). The results of our analysis with uncertain demand indicate that the developed model provides robust solutions when actual demand shifts from the predicted

values. Our analysis shows that there can be high-cost savings by using the proposed multi-period model as compared with a static counterpart.

While the focus of our study is COVID-19, testing plays a significant role in the control of other infectious diseases and the developed model can be applied to those as well. Based on the reported outbreaks in recent years, the frequency of infectious disease outbreaks is expected to increase in the future [28]. Since these outbreaks are inevitable, proactive actions to improve our readiness should be studied now. In this context, the model can be used or extended to develop response plans for future infectious disease outbreaks (e.g., monkeypox), especially for those that use PCR tests with a similar diagnostic process (i.e., specimen collection plus laboratory analysis) [2, 53]. In case of a future pandemic, the developed model may help control the spread of the disease at the early stages of the pandemic by proactively managing testing capacity to avoid the challenges and difficulties we have had since the beginning of the COVID-19 pandemic.

The developed model can be extended in several directions. First, since lab capacity is not binding in our study, we do not include the decisions regarding the capacity expansions for the labs. A natural extension could be to allow for the capacity expansions of the labs as well. We obtain the optimal results for our case study using a commercially available solver in very reasonable times, hence, we did not develop any specialized algorithms. In future research, decomposition methodologies, heuristic and metaheuristic algorithms can be developed and employed to effectively solve large-sized instances of the problem. In addition, testing center locations and capacities may impact the disease spread, and hence, the future demand patterns in the long run. In future research, our optimization model can be embedded with an SEIR model through a feedback mechanism to better capture the effects of location and capacity expansion decisions on demand, and to incorporate the effects of various factors, such as disease prevalence, variants, vaccination, and test compliance [38, 49]. The resulting modeling approach would yield more resilient decisions and improve the practicality and applicability of the insights derived from model outcomes.

Acknowledgements

We gratefully acknowledge the comments and suggestions of the knowledge users from the Ontario Ministry of Health and the Challenge Questions Initiative. We would like to thank in particular Elizabeth Chiu, Jason Apostolopoulos, and Pavlina Faltynek from the Challenge Questions Initiative for their valuable and insightful suggestions and contributions. We also thank Ewan Simms for his help with data collection and visualization and the Grand River Hospital laboratory. This research was supported by the Natural Sciences and Engineering Research Council of Canada (NSERC) with grants RGPIN-2022-03523 and RGPIN-2018-06596.

References

- [1] Aboolian, R., Berman, O., and Krass, D. (2012). Profit maximizing distributed service system design with congestion and elastic demand. *Transportation Science*, 46(2):247–261.
- [2] Adler, H., Gould, S., Hine, P., Snell, L. B., Wong, W., Houlihan, C. F., Osborne, J. C.,

- Rampling, T., Beadsworth, M. B., Duncan, C. J., et al. (2022). Clinical features and management of human monkeypox: a retrospective observational study in the UK. *The Lancet Infectious Diseases* (in press).
- [3] Ahmadi-Javid, A., Seyedi, P., and Syam, S. S. (2017). A survey of healthcare facility location. *Computers & Operations Research*, 79:223–263.
- [4] Alumur, S. A., Nickel, S., Rohrbeck, B., and Saldanha-da Gama, F. (2018). Modeling congestion and service time in hub location problems. *Applied Mathematical Modelling*, 55:13–32.
- [5] Baker, J. (2022). New COVID-19 assessment centres opening in Waterloo Region to ease hospital pressures—Kitchener CTV News. <https://kitchener.ctvnews.ca/new-covid-19-assessment-centres-opening-in-waterloo-region-to-ease-hospital-pressures-1.5739165>. [Online; accessed 01-March-2022].
- [6] Barrett, K., Khan, Y. A., Mac, S., Ximenes, R., Naimark, D. M., and Sander, B. (2020). Estimation of COVID-19 induced depletion of hospital resources in Ontario, Canada. *Canadian Medical Association Journal*, 192(24):E640–E646.
- [7] Batun, S. and Begen, M. A. (2013). Optimization in healthcare delivery modeling: Methods and applications. In *Handbook of Healthcare Operations Management*, pages 75–119. Springer.
- [8] Böger, B., Fachi, M. M., Vilhena, R. O., Cobre, A. F., Tonin, F. S., and Pontarolo, R. (2021). Systematic review with meta-analysis of the accuracy of diagnostic tests for COVID-19. *American Journal of Infection Control*, 49(1):21–29.
- [9] Brown, D. (2020a). Line ups and long wait times as demand for COVID-19 tests increases in Waterloo Region—Kitchener CTV news. <https://kitchener.ctvnews.ca/line-ups-and-long-wait-times-as-demand-for-covid-19-tests-increases-in-waterloo-region-1.5108000>. [Online; accessed 01-May-2021].
- [10] Brown, D. (2020b). Why you can’t get that COVID-19 test result back in 24 hours — CBC News. <https://www.cbc.ca/news/canada/kitchener-waterloo/covid-test-results-turnaround-waterloo-region-1.5709795>. [Online; accessed 01-May-2021].
- [11] Bueckert, K. (2020). More COVID-19 testing capacity coming to Waterloo Region as demand remains high—CBC News. <https://www.cbc.ca/news/canada/kitchener-waterloo/testing-demands-covid-19-waterloo-region-1.5660690>. [Online; accessed 01-May-2021].
- [12] Campbell, J. R., Uppal, A., Oxlade, O., Fregonese, F., Bastos, M. L., Lan, Z., Law, S., Oh, C. E., Russell, W. A., Sulis, G., et al. (2020). Active testing of groups at increased risk of acquiring SARS-CoV-2 in Canada: costs and human resource needs. *Canadian Medical Association Journal*, 192(40):E1146–E1155.
- [13] Case study data (2022). <https://docs.google.com/spreadsheets/d/1KFS8Cysv3FL3k5IYMrQ-u1rLC3zGVYMG/edit?usp=sharing&oid=105869416816418630273&rtpof=true&sd=true>.
- [14] Cui, Y., Ni, S., and Shen, S. (2021). A network-based model to explore the role of testing in the epidemiological control of the COVID-19 pandemic. *BMC Infectious Diseases*, 21(1):1–12.
- [15] Daskin, M. S. and Dean, L. K. (2004). Location of health care facilities. In *Operations Research and Health Care: A Handbook of Methods and Applications*, pages 43–76. Springer.
- [16] Davari, S., Kilic, K., and Ertek, G. (2015). Fuzzy bi-objective preventive health care network design. *Healthcare Management Science*, 18(3):303–317.

- [17] DeClerq, K. (2021). Ontario residents waiting days to get COVID-19 test, resulting in potential discrepancy in reported cases—Toronto CTV News. <https://toronto.ctvnews.ca/ontario-residents-waiting-days-to-get-covid-19-test-resulting-in-potential-discrepancy-in-reported-cases-1.5714536>. [Online; accessed 01-March-2022].
- [18] Dogan, K., Karatas, M., and Yakici, E. (2019). A model for locating preventive health care facilities. *Central European Journal of Operations Research*, pages 1–31.
- [19] Elhedhli, S. (2006). Service system design with immobile servers, stochastic demand, and congestion. *Manufacturing & Service Operations Management*, 8(1):92–97.
- [20] Elhedhli, S. and Hu, F. X. (2005). Hub-and-spoke network design with congestion. *Computers & Operations Research*, 32(6):1615–1632.
- [21] Garey, M. R. and Johnson, D. S. (1979). *A Guide to the Theory of NP-completeness. Computers and intractability*, volume 174. Freeman San Francisco, CA.
- [22] Ghaderi, A. and Jabalameli, M. S. (2013). Modeling the budget-constrained dynamic uncapacitated facility location–network design problem and solving it via two efficient heuristics: a case study of health care. *Mathematical and Computer Modelling*, 57(3-4):382–400.
- [23] Government of Canada (2020). Fiscal summary - Canada.ca. <https://www.canada.ca/en/departement-finance/economic-response-plan/fiscal-summary.html>. [Online; accessed 01-May-2021].
- [24] Government of Ontario (2020). Testing volumes and results. <https://covid-19.ontario.ca/data/testing-volumes-and-result>. [Online; accessed 15-September-2021].
- [25] Gu, W., Wang, X., and McGregor, S. E. (2010). Optimization of preventive health care facility locations. *International Journal of Health Geographics*, 9(1):1–16.
- [26] Güneş, E. D., Melo, T., and Nickel, S. (2019). Location problems in healthcare. In *Location Science*, pages 657–686. Springer.
- [27] Güneş, E. D. and Örmeci, E. L. (2018). OR applications in disease screening. In *Operations Research Applications in Health Care Management*, pages 297–325. Springer.
- [28] Houlihan, C. F. and Whitworth, J. A. (2019). Outbreak science: recent progress in the detection and response to outbreaks of infectious diseases. *Clinical Medicine*, 19(2):140.
- [29] Intrevado, P., Verter, V., and Tremblay, L. (2019). Patient-centric design of long-term care networks. *Health Care Management Science*, 22(2):376–390.
- [30] Jena, S. D., Cordeau, J.-F., and Gendron, B. (2015). Dynamic facility location with generalized modular capacities. *Transportation Science*, 49(3):484–499.
- [31] Li, X. (2023). A two-level policy for controlling an epidemic and its dynamics. *Omega*, 115:102753.
- [32] Li, Y., Wen, X., Choi, T.-M., and Chung, S.-H. (2022). Optimal establishments of massive testing programs to combat COVID-19: A perspective of parallel-machine scheduling-location (ScheLoc) problem. *IEEE Transactions on Engineering Management*.
- [33] Liu, K., Liu, C., Xiang, X., and Tian, Z. (2021). Testing facility location and dynamic capacity planning for pandemics with demand uncertainty. *European Journal of Operational Research (in press)*.

- [34] Manabe, Y. C., Sharfstein, J. S., and Armstrong, K. (2020). The need for more and better testing for COVID-19. *The Journal of the American Medical Association*, 324(21):2153–2154.
- [35] Miller, A. (2022). Canada is flying blind with omicron as COVID-19 testing drops off a cliff — CBC News. <https://www.cbc.ca/news/health/omicron-testing-canada-cases-hospitalizations-po-1.6304195>. [Online; accessed 04-February-2022].
- [36] Ndiaye, M. and Alfares, H. (2008). Modeling health care facility location for moving population groups. *Computers & Operations Research*, 35(7):2154–2161.
- [37] Nickel, S. and Saldanha-da Gama, F. (2019). Multi-period facility location. In *Location Science*, pages 303–326. Springer.
- [38] Ogden, N. H., Fazil, A., Arino, J., Berthiaume, P., Fisman, D. N., Greer, A. L., Ludwig, A., Ng, V., Tuite, A. R., Turgeon, P., et al. (2020). Artificial intelligence in public health: Modelling scenarios of the epidemic of COVID-19 in Canada. *Canada Communicable Disease Report*, 46(8):198.
- [39] Ontario Health (2020a). COVID-19 Test Collection and Analysis. <https://www.ontariohealth.ca/COVID-19/testing-analysis>. [Online; accessed 18-May-2021].
- [40] Ontario Health (2020b). COVID-19 Testing and Lab Processing Update. <https://www.ontariohealth.ca/sites/ontariohealth/files/2020-10/OH-Memo-COVID-19-testing-and-lab-processing-2020-10-09.pdf>. [Online; accessed 18-May-2021].
- [41] Ontario Ministry of Health (2020). Guidance for the health sector. https://www.health.gov.on.ca/en/pro/programs/publichealth/coronavirus/2019_guidance.aspx. [Online; accessed 11-December-2021].
- [42] Public Health Ontario (2020). Ontario public health system. <https://www.publichealthontario.ca/en/About/News/2020/Ontario-Public-Health-System>. [Online; accessed 18-May-2021].
- [43] Public Health Ontario (2022). COVID-19 Data and Surveillance. <https://www.publichealthontario.ca/en/data-and-analysis/infectious-disease/covid-19-data-surveillance>. [Online; accessed 13-November-2022].
- [44] Rais, A. and Viana, A. (2011). Operations research in healthcare: a survey. *International Transactions in Operational Research*, 18(1):1–31.
- [45] Ramirez-Nafarrate, A., Lyon, J. D., Fowler, J. W., and Araz, O. M. (2015). Point-of-dispensing location and capacity optimization via a decision support system. *Production and Operations Management*, 24(8):1311–1328.
- [46] Saveh-Shemshaki, F., Shechter, S., Tang, P., and Isaac-Renton, J. (2012). Setting sites for faster results: Optimizing locations and capacities of new tuberculosis testing laboratories. *IIE Transactions on Healthcare Systems Engineering*, 2(4):248–258.
- [47] Schaffer, A. L., Dobbins, T. A., and Pearson, S.-A. (2021). Interrupted time series analysis using autoregressive integrated moving average (ARIMA) models: a guide for evaluating large-scale health interventions. *BMC Medical Research Methodology*, 21(1):1–12.
- [48] Tang, L., Li, Y., Bai, D., Liu, T., and Coelho, L. C. (2022). Bi-objective optimization for a multi-period COVID-19 vaccination planning problem. *Omega*, 110:102617.
- [49] Tuite, A. R., Fisman, D. N., and Greer, A. L. (2020). Mathematical modelling of COVID-19 transmission and mitigation strategies in the population of Ontario, Canada. *Canadian Medical Association Journal*, 192(19):E497–E505.

- [50] Verter, V. and Lapierre, S. D. (2002). Location of preventive health care facilities. *Annals of Operations Research*, 110(1):123–132.
- [51] Verter, V. and Zhang, Y. (2015). Location models for preventive care. In *Applications of Location Analysis*, pages 223–241. Springer.
- [52] Vidyarthi, N. and Kuzgunkaya, O. (2015). The impact of directed choice on the design of preventive healthcare facility network under congestion. *Health Care Management Science*, 18(4):459–474.
- [53] Yang, S. and Rothman, R. E. (2004). PCR-based diagnostics for infectious diseases: uses, limitations, and future applications in acute-care settings. *The Lancet Infectious Diseases*, 4(6):337–348.
- [54] Zauli, D. A. G. (2019). PCR and infectious diseases. In *Synthetic Biology-New Interdisciplinary Science*, pages 137–145. IntechOpen.
- [55] Zhang, C., Li, Y., Cao, J., and Wen, X. (2022). On the mass COVID-19 vaccination scheduling problem. *Computers & Operations Research*, 141:105704.
- [56] Zhang, Y., Berman, O., Marcotte, P., and Verter, V. (2010). A bilevel model for preventive healthcare facility network design with congestion. *IIE Transactions*, 42(12):865–880.
- [57] Zhang, Y., Berman, O., and Verter, V. (2009). Incorporating congestion in preventive healthcare facility network design. *European Journal of Operational Research*, 198(3):922–935.
- [58] Zhang, Y., Berman, O., and Verter, V. (2012). The impact of client choice on preventive healthcare facility network design. *OR Spectrum*, 34(2):349–370.

Supplementary Materials

Table 5 presents the optimal solutions under additional demand scenarios with min-cost formulation when all demand has to be satisfied on time, i.e., the number of delayed appointments is zero. The first and second columns of the table show the demand week and the percent increase in the demand, respectively. The third and fourth columns specify the average number and utilization of pop-up testing centers opened. The fifth and sixth columns show the average capacity expansion and utilization for existing centers during the planning horizon. The seventh column presents the optimum objective function value (i.e., total cost). Finally, the last column reports the solution time of the model with CPLEX. The first row for each demand set corresponds to the base case results discussed in Section 5.1.

For the low demand week, compared to the base case, the model does not open additional pop-up testing centers until the demand is increased by 50%, i.e., the increase in testing demand can be served by using the base case pop-up center and expanding the capacity of the existing assessment centers. For instance, for the 30% demand increase in the low demand week, the model opens the base case pop-up center and expands the capacity of an existing one by 25.3% rather than opening two pop-up centers to avoid a larger fixed cost. For medium and high demand weeks, the average number of opened pop-up testing centers increases with demand. There are several instances (e.g., 30% for high demand week) in which the model prefers using pop-up testing centers over the capacity expansion of the existing ones due to lower unit testing cost. In general, the total cost increases as the overall testing demand increases. The solution times are generally greater for higher demand values of the same demand set and greater for the high demand week from December.

Table 6 presents the results with different maximum travel distances. All instances in Table 6 are solved optimally within 8 minutes. The solution times generally increase as the demand level and maximum travel time increase. When the maximum travel distance increases, more people can get access to testing from a particular existing or pop-up testing center. This results in opening fewer pop-up testing centers, as existing capacity can be better utilized to serve remote demand, as well as an increase in the average utilization of the opened pop-ups. On the other hand, when the maximum travel distance decreases, more pop-up testing centers are needed which may lead to lower utilization of some pop-up testing centers. For instance, if the maximum travel distance is decreased to 5 km, pop-ups have a pretty low utilization (e.g., 11% under low demand scenario).

Table 5: Model outputs under different demand scenarios.

Demand set	Demand level	Avg # of opened pop-ups	Avg utilization of pop-ups (%)	Avg capacity expansion for existing centers (%)	Avg utilization of existing centers (%)	Min total cost(\$)	Solution time (sec)
December (high)	Base case	3	80.9	19.2	71.3	864,513	41.8
	+10%	4	79.6	25	65.7	962,564	41.2
	+20%	4.8	78.7	29	49.7	1,052,885	20
	+30%	5	78.9	18.3	58.8	1,150,867	26
	+40%	6	77.6	18	50.9	1,240,367	22.7
	+50%	7	75.3	17	50.5	1,345,079	237.6
April (medium)	Base case	1.8	76.3	0	58.5	583,731	20
	+10%	2	78.7	10	60.3	648,831	18.7
	+20%	2	80.5	17.5	70.4	698,525	24.4
	+30%	2.3	80.9	19.2	72.9	762,655	34.7
	+40%	2.7	81.1	15.6	69.8	823,957	34.9
	+50%	3.3	81	23.9	899,370	42.4	
August (low)	Base case	1	89.3	0	37.3	320,672	1.2
	+10%	1	90.1	10	39.4	352,877	9.6
	+20%	1	92.5	23.3	43	381,653	13.7
	+30%	1	94.6	25.3	48.5	421,403	19
	+40%	1	95.7	25.7	52	449,362	12.9
	+50%	1.8	78.7	31.1	497,235	18	

Table 6: Solutions of the model for different maximum travel distances under different demand scenarios

Demand set	Maximum travel distance (km)	Average # of opened pop-ups	Avg utilization of pop-ups (%)	Avg capacity expansion for existing centers (%)	Avg utilization of existing centers (%)	Min total cost(\$)	Solution time (sec)
December (high)	5	14	27.5	0	26.4	1,040,807	1.7
	10	6.8	41.9	34	59.9	926,964	21.3
	15	4	61.4	12.1	72.9	879,739	32.2
	20 (Base case)	3	80.9	19.2	71.3	864,513	41.8
	25	3	82.7	17.4	67	864,727	42.2
	30	3	82.9	15.5	61.9	864,693	120.4
April (medium)	5	13.7	20.1	0	19.5	776,223	1.8
	10	5.8	31.3	0	46.9	649,740	1.7
	15	3	50.8	0	50.9	603,062	16.9
	20 (Base case)	1.8	76.3	0	58.5	583,731	20
	25	1.3	82.2	12.1	68.1	576,088	16.8
	30	1.3	81.9	12.5	65.1	576,063	492.3
August (low)	5	12	11	10	43.7	498,107	1
	10	5	26.3	22.8	38.2	386,318	1.5
	15	2	47	25	32.9	341,029	6.2
	20 (Base case)	1	89.3	0	37.3	320,672	1.2
	25	1	92.6	0	21.4	319,934	1.3
	30	1	92.8	0	14.6	319,889	1.6